Article

Not peer-reviewed version

Advantages of Long Wavelength Photosensitizer *meso*-Tetra(3-Pyridyl) Bacteriochlorin in Therapy of Bulky Tumors

Ekaterina A. Plotnikova , Elena Nemtsova * , Maxim A. Abakumov , Andrei Pankratov , Peter Shegai , Andrey Kaprin

Posted Date: 9 November 2023

doi: 10.20944/preprints202311.0582.v1

Keywords: photodynamic therapy; photosensitizer; bacteriochlorins; photocytotoxicity; photoinduced antitumor activity; cell; tissue; tumor

Article

Advantages of Long Wavelength Photosensitizer *meso*-Tetra(3-pyridyl) Bacteriochlorin in Therapy of Bulky Tumors

Ekaterina Plotnikova [1,2], Elena Nemtsova [1,*], Maxim Abakumov [3], Andrey Pankratov [1,2], Peter V. Shegai [1] and Andrey Kaprin [1]

[1] Moscow Hertsen Research Institute of Oncology —Branch of the FSBI "National Medical Research Radiology Centre" of the Ministry of Health of the Russian Federation, 3, 2nd Botkinskiy pr, Moscow125284, Russia; plotnikovaekaterina62@gmail.com (E.P.); nemtz@yandex.ru (E.N.); andreimnioi@yandex.ru (A.P.); dr.shegai@mail.ru (P.S.); kaprin@mail.ru (A.K.)

[2] Institute of Fine Chemical Technologies, MIREA-Russian Technological University, 119571 Moscow, Russia; plotnikovaekaterina62@gmail.com (E.P.); andreimnioi@yandex.ru (A.P.)

[3] Pirogov Russian National Research Medical University, 117997 Moscow, Russia; abakumov1988@gmail.com (M.A.)

* Correspondence: nemtz@yandex.ru

Abstract: The research presents a novel synthetic photosensitizer for photodynamic therapy (PDT) of malignant tumors - meso-tetra(3-pyridyl) bacteriochlorin, which absorbs at 747 nm (in the long-wavelength region of the spectrum) and is stable when stored in the dark. H_2Py_4BC demonstrates pronounced photoinduced activity *in vitro* against tumor cells of various genesis (IC_{50} varies from 21 to 68 nM for HEp2, EJ, S37, CT26, and LLC cultured cells) and provides *in vivo* pronounced antitumor efficacy in the treatment of mice bearing small or large S37, Colo26, and LLC metastatic tumors, as well as in the treatment of rats bearing RS-1 liver cholangioma. As a result, total regress of primary tumor nodules and cure of 40 to 100% of the animals were proved by the experiment criteria, MRI, and histological analysis. Meso-tetra(3-pyridyl) bacteriochlorin quickly penetrates and accumulates in the tumor tissue and internal organs of mice, and after 24 hours 80% of the dye is excreted from skin as well as 87% - 92% from liver, kidneys, and spleen.

Keywords: photodynamic therapy; photosensitizer; bacteriochlorins; photocytotoxicity; photoinduced antitumor activity; cell; tissue; tumor

1. Introduction

Photodynamic therapy (PDT) is an advanced minimum invasive anticancer method of therapy which is based on administration of photosensitizers (PS) mainly accumulated in target tissues. Upon light activation they produce reactive singlet oxygen damaging tumor cells [1–4].

The clinical PDT progress encourages researchers to develop new advanced PSs, especially those absorbing in the red/near-infrared (NIR) biological transparency window (λ_{max} at 700–800 nm). Own light absorption of biological tissues in this window is minimal thus allowing deeper light penetration through the tissue and, as a result, the higher therapeutic effect. There is an increasing interest in bacteriochlorin-based photosensitizers as fluorescent probes and medicines for diagnostics and treatment, because their NIR fluorescence and efficient singlet oxygen generation are advantageous both for imaging and photodynamic therapy [4–10]. The most important characteristics of these PSs are their rapid clearance from circulation and minimum skin phototoxicity induced by visible light. Modern clinical trials of Redaporfin and TOOKAD , the bacteriochlorin-based preparations, indicate the prospects of using PSs which absorb in the long-wavelength region of the spectrum.

Preprints (www.preprints.org) | NOT PEER-REVIEWED | Posted: 9 November 2023 doi:10.20944/preprints202311.0582.v1

Recently we have synthesized new water-soluble tetra- and octacationic bacteriochlorins using *meso*-tetra(3-pyridyl)bacteriochlorin (H_2Py_4BC) as the starting compound with pro-cationic pyridine moiety [17,18]. Tetracationic derivatives ## 1-3 (Figure 1) have been synthesized by alkylation of H_2Py_4BC with 1,4-dibromobutane, 1,2-dibromoethane, or heptyl bromide, respectively. Tetracationic bacteriochlorins 1 and 2 with the terminal bromine atoms in their side alkyl chains were converted into octacationic derivatives ## 4-6 (Figure 1) by treating with an excess of pyridine (4,5) or N,N-dimethylaminoethanol (6).

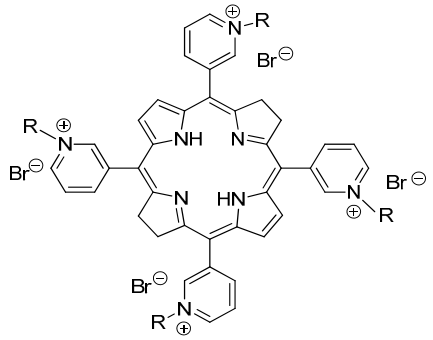

R = $(CH_2)_4Br$(1); $(CH_2)_2Br$(2); C_7H_{15} (3); $(CH_2)_4$-$\overset{\oplus}{N}C_6H_5$ $\overset{\ominus}{Br}$(4); $(CH_2)_2$-$\overset{\oplus}{N}C_6H_5$ $\overset{\ominus}{Br}$ (5); $(CH_2)_4$-$\overset{\oplus}{N}(CH_3)_2CH_2CH_2OH$ $\overset{\ominus}{Br}$ (6)

Figure 1. The structures of tetra- and octacationic derivatives of *meso*-tetra(3-pyridyl)bacteriochlorin (H_2Py_4BC).

All of the synthesized bacteriochlorins' molecules possess intense band at 747-761 nm in the NIR spectral region. They are highly stable in aqueous solutions and do not show any sign of aggregation. *In vitro* and *in vivo* studies of the specific antitumor activity of H_2Py_4BC and its cationic derivatives ## 1, 4, and 6 have shown pronounced dark stability and phototoxicity inducing cure in near 100 % of animals [3,20,21]. H_2Py_4BC demonstrated the fastest elimination from the animal body and, accordingly, the decreased skin phototoxicity. Bacteriosens, its water-soluble formulation containing Colliphor ELP, mannitol, and citric acid, successfully completed preclinical studies [22]. Moreover, the positive charge of bacteriochlorin derivatives ## 1-5 was highly efficient in photodynamic inactivation both of gram-positive bacteria S. aureus and gram-negative bacteria P. aeruginosa, as well as their biofilms [23–26].

This work presents the results of evaluation of the long wavelength bacteriochlorin-based H_2Py_4BC photosensitizer and demonstrates its benefits for treatment of the bulky tumors in comparison with Radachlorin® [27].

2. Results and Discussion

2.1. Spectral properties of meso-tetra(3-pyridyl)bacteriochlorin

H_2Py_4BC in the aqueous solution with low content of Cremophor (0.05%) demonstrates maximal absorption at 356, 379, 521, and 683 nm as well as at 747 nm within the long wavelength area (Figure 2a).

Maximal fluorescence of H_2Py_4BC under the same conditions was detected at 754±2 nm (Figure 2b). Comparative study of fluorescence spectra of H_2Py_4BC solution with 0.4 mg/ml concentration performed *ex tempore* and after 1 or 6 months of shelf storage in the dark did not reveal the Q-band displacement or significant decrease of fluorescence intensity and thus demonstrated PS stability.

Preprints (www.preprints.org) | NOT PEER-REVIEWED | Posted: 9 November 2023 doi:10.20944/preprints202311.0582.v1

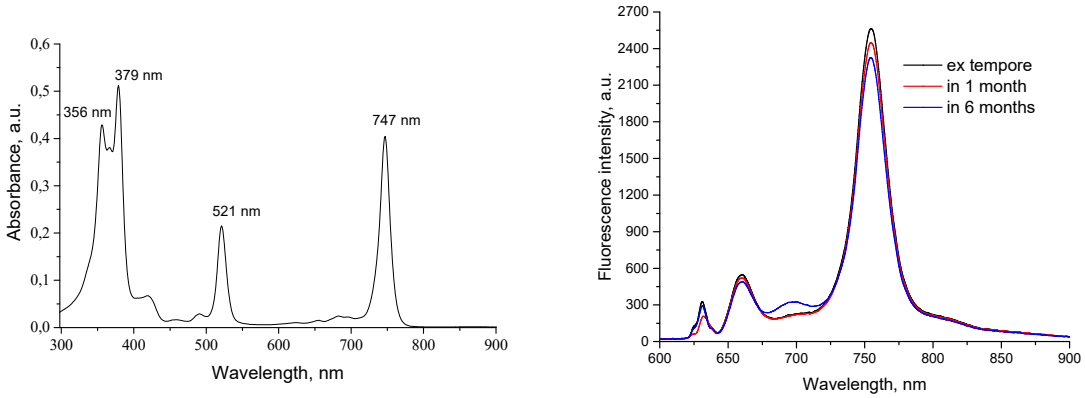

(**a**) (**b**)

Figure 2. Absorption (a) and fluorescence (b) spectra of H_2Py_4BC in 4% Cremophor solution. The concentration of the dye is 5 μg/ml.

2.2. In vitro study of PS photo- and cytotoxicity

Maximum phototoxicity after irradiation of the cultured Hep2 and EJ human tumor cells in the presence of H_2Py_4BC was detected after six-hour incubation of the cells with the PS (IC_{50} was 26.1±2.2 nM and 30.4±3.3 nM, respectively) whereas IC_{50} was 69.1±3.6 nM and 22.4±2.1 nM for the S37 and LLC murine tumor cells, respectively, incubated under the same conditions; IC_{50} for the murine CT26 carcinoma was 21.4±1.5 nM after two-hour incubation with the dye (Figure 3a,b).

Changing the incubation medium comprising H_2Py_4BC for a fresh medium without the dye before the light impact did not influence the intensity of cytotoxic effect for Hep2, EJ, and C26 cells, but caused some decrease of photoinduced toxicity for S37 and LLC cells even when the incubation time was extended beyond the time necessary to achieve the maximum effect (Figure 3).

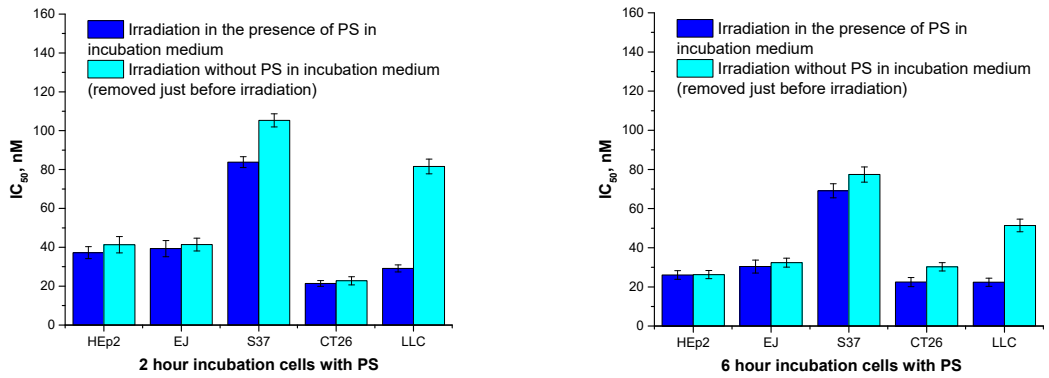

(**a**) (**b**)

Figure 3. Photoinduced H_2Py_4BC activity with and without depletion of the dye before the irradiation: a – 2 hour incubation; b – 6 hour incubation.

So, the differences in the PDT cytotoxicity for the studied cell cultures under various conditions may be accounted for both the variations in the rate of the dye accumulation/elimination *in vitro* and the different sensitivity of the cells to the photoinduced damage. It should be noted that *meso*-tetra(3-pyridyl)bacteriochlorin after 24-hour incubation without irradiation had no phototoxic impact on human or murine cells (Figure 4).

Preprints (www.preprints.org) | NOT PEER-REVIEWED | Posted: 9 November 2023 doi:10.20944/preprints202311.0582.v1

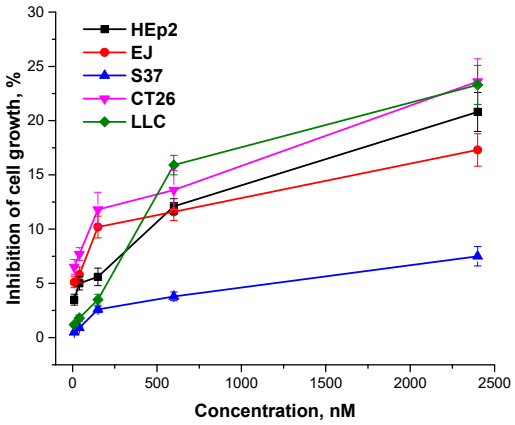

Figure 4. Dark cytotoxicity of *meso*-tetra(3-pyridyl)bacteriochlorin versus its concentration.

2.3. In vivo study

2.3.1. Biodistribution of meso-tetra(3-pyridyl)bacteriochlorin in organs and tissues of tumor-bearing animals

In vivo optical imaging in S37-bearing mice has demonstrated that increased accumulation (in comparison with the adjacent tissues) of the intravenously infused H_2Py_4BC was observed in tumor nodules located on a murine paw (Figure 5).

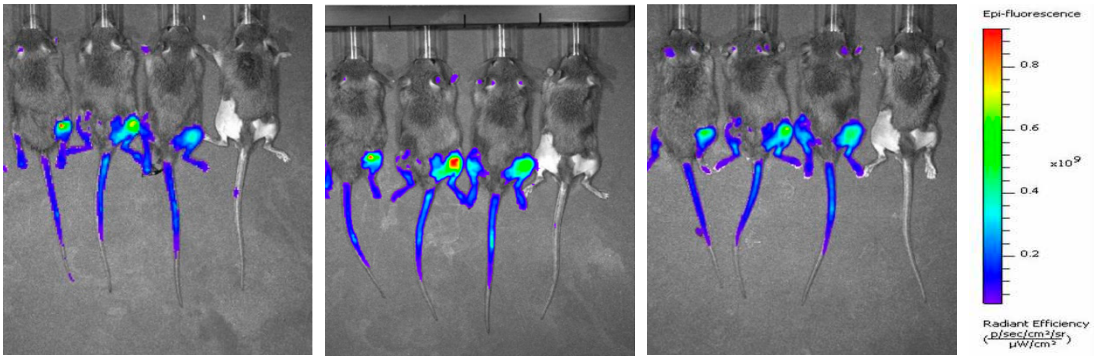

(**a**) (**b**) (**c**)

Figure 5. *In vivo* fluorescence imaging of mice with subcutaneously inoculated S37 sarcoma at various periods after the intravenous administration of H_2Py_4BC: A – after 15 min, B – after 2 hours, C – after 24 hours. Imaging: three mice with the dye (to the left), fourth mouse - control without the dye. Imaging was performed using IVIS Spectrum-CT device.

Quantitative data processing showed that the most intensive fluorescence (7.4 – 8.6 photon/sec/cm^2) was recorded at the earliest periods of observation (15 minutes – 2 hours after the intravenous H_2Py_4BC infusion). According to the analysis of fluorescent imaging, the maximum fluorescence contrast between tumor and adjacent skin (FCt/sk) was as much as 3.3±0.2 in 15 minutes after the infusion. Local spectroscopy demonstrated that the high level of H_2Py_4BC normalized fluorescence (NF) in S37 tumor tissue was observed in 5 minutes after the intravenous infusion of the dye. It reached its maximum in 15 min after the impact (5.5±0.2 r.u.) and maintained a relatively high level for 2 hours after the dye infusion (Figure 6). In 24 hours after the H_2Py_4BC administration NF in tumor tissue was not more than 7% of the maximum value.

Preprints (www.preprints.org) | NOT PEER-REVIEWED | Posted: 9 November 2023 doi:10.20944/preprints202311.0582.v1

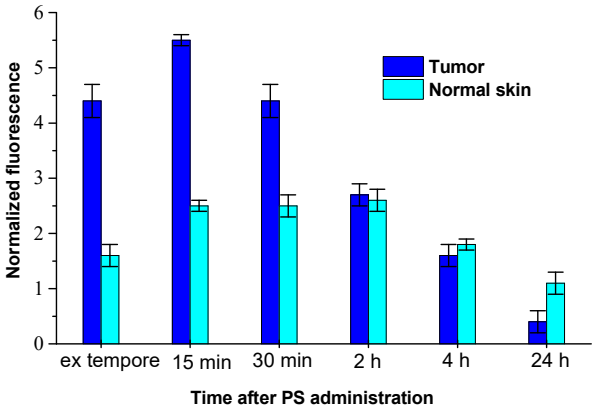

Figure 6. Normalized fluorescence (λ_{max} 747 nm) in tumor and in normal skin of mice bearing subcutaneously inoculated S37 sarcoma at various periods after H_2Py_4BC intravenous administration. Results of *ex vivo* local fluorescence spectroscopy performed using LESA-06 device.

In normal skin the increased content of H_2Py_4BC was detected during the time interval from 15 min till 4 hours after the infusion, the NF level achieved 2.6±0.1 r.u. The maximum FCt/sk for H_2Py_4BC (2.5±0.3) was detected in 5 till 15 min after the dye infusion. Analysis of fluorescence signals obtained *ex vivo* from the inner organs and tissues of the studied animals by the contact method has shown that the maximum content of the fluorescent form of H_2Py_4BC was determined in blood (11.5±0,3 r.u.) at the initial periods of observation (5 min after the intravenous dye infusion). It decreased 4 hours later to 5.2% of the initially registered level, and in 24 hours the dye could not be detected in blood. Similar dynamics of NF level was observed in the spleen.

The NF in animal liver became significantly higher than in the blood (21.9±0.7) as quickly as 5 min after H_2Py_4BC infusion, in kidneys its level was comparable with that in the blood (9.5±0.4) at that time, and within 15 min it achieved maximum levels both in the liver and kidneys (32.6±0.9 and 14.1±0.6, respectively). NF in the liver and in the kidneys decreased gradually within 4 hours after the H_2Py_4BC infusion to 58.6% and 51.8% of the maximum levels detected in these organs, and in 24 hours it was 16.3% and 12.6% of the maximum values. In spleen the fluorescent form of the dye was detected during 24 hours after H_2Py_4BC administration, in kidneys – up to 2 days, and in liver the residual amount of the dye was observed up to the 5th day (Figure 7).

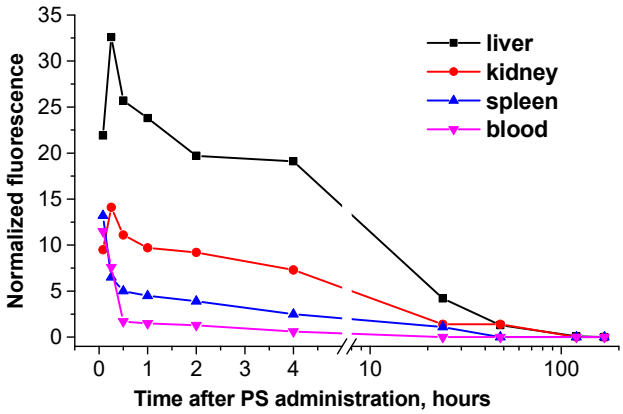

Figure 7. Normalized fluorescence in blood and inner organs of mice after intravenous administration of H_2Py_4BC. Data were obtained *ex vivo* by local fluorescence spectroscopy.

 doi:10.20944/preprints202311.0582.v1

The obtained data showed fast distribution and elimination of H_2Py_4BC from mouse body after its intravenous administration. The elimination predominantly took place through the excretory systems of kidneys and liver.

Fifteen minutes after i/v infusion of H_2Py_4BC $FC_{t/sk}$ in mice with subcutaneously inoculated LLC or CT26 was 2.8±0.2 and 3.0±0.3, respectively. The dynamics of NF in blood, liver, kidneys, and spleen was similar to that in S37-bearing animals.

2.3.2. Photoinduced antitumor activity of meso-tetra(3-pyridyl)bacteriochlorin and Radachlorin in the models of transplanted murine tumors

First of all, in a set of multiparameter experiments performed with H_2Py_4BC and Radachlorin as PSs for small tumors, optimal regimens for antitumor PDT have been worked out. For this purpose we varied doses of each PS - from 0.5 to 7.5 mg/kg, intervals between the infusion of PS and the beginning of the light impact – from 5 min to 4 hours, and power density of irradiation in mono-positional regimen – from 90 to 270 J/cm^2. As a result, the dye doses and light impact regimens that caused the most pronounced antitumor efficacy without adverse events in S37 sarcoma model were developed (Table 1).

Neither death of animals nor any difference in the condition of the photoinduced edema of the paw (the edema became smaller within 4 days) were observed after PDT under these conditions.

The comparative study in optimal mono- and poly-positional radiation regimens was performed to estimate the efficacy of H_2Py_4BC and Radachlorin for antitumor PDT in the models of murine S37, CT26, and LLC tumors of various volumes.

The analysis of the obtained data has shown that under optimal conditions PDT with both H_2Py_4BC and Radachlorin is highly efficient against all of the studied small tumors. The inhibition of tumor growth and survival of animals persisted over the entire period of observation at the 100% level when the long wavelength PS was used (Table 2). The administration of Radachlorin as a PS in its optimal regimen on the 20th day after PDT resulted in 98.2%, 100%, and 95.2% tumor growth inhibition for S37, CT26, and LLC, respectively (Table 2).

Table 1. Optimal therapeutic regimens of H_2Py_4BC and Radachlorin-mediated photodynamic therapy in a subcutaneous model of murine S37 sarcoma.

PDT conditions	Photosensitizer	
	H_2Py_4BC	**Radachlorin**
PS dose, μM/kg	3.2	7.6
Δt, min	30	15
Light impact:		
LED source, λ (nm)	740 ± 28	662 ± 14
Power density, mW/cm^2	100 ± 3	100 ± 4
Energy density, J/cm^2	90	90

By the 20th day tumors in the untreated animals achieved the volumes of 2350 mm^3, 2450mm^3, and 2200 mm^3 for S37, CT26, and LLC, respectively. It has to be noted that the life span of the mice bearing metastatic transplanted tumors is restricted by the progressive growth of metastatic nodes. Taking into account the decline of the animals' condition and the humane considerations, the 20th day after PDT was considered to be the end point of the observation. Animals were subjected to forced euthanasia. Mean tumor volumes after PDT were 92.6±92.6, 0 and 206±206 mm^3 for S37, CT26, and LLC, respectively. Animals without visible growth of primary tumor nodules on the date of euthanasia were observed for 90 days. After this period the survived animals were also euthanized.

Preprints (www.preprints.org) | NOT PEER-REVIEWED | Posted: 9 November 2023 doi:10.20944/preprints202311.0582.v1

There were no signs of further tumor growth and metastasis, so these animals were considered to be cured.

Table 2. Antitumor efficacy of PDT with meso-tetra (3-pyridyl) bacteriochlorin and Radachlorin in mice with small tumors of various histogenesis (Vt=130±30 mm^3).

PS	Tumor growth inhibition (ITG), %					RR, %
	7 day	10 day	14 day	17 day	20 day	
S37 sarcoma						
Radachlorin	100	100	100	100	98,2	80
H_2Py_4Bc	100	100	100	100	100	100
CT26 carcinoma						
Radachlorin	100	100	100	100	100	100
H_2Py_4Bc	100	100	100	100	100	100
LLC carcinoma						
Radachlorin	100	100	98,3	96,2	95,2	60
H_2Py_4Bc	100	100	100	100	100	100

Total regression of the primary tumor nodules was observed in all studied models (S37, LLC, and CT26) when H_2Py_4BC-mediated PDT was performed in animals bearing large tumors using the previously developed regimen parameters and poly-positional radiation (2,0 mg/kg dose, 740±28 nm LED, and 270 J/cm^2 total dose) (Figure 8).

The efficiency of PDT with Radachlorin® (5.0 mg/kg dose, 662±14 nm LED, 270 J/cm^2 total dose) was significantly lower: TGI on the 20th day after the treatment was 37% in the S37 model, 60% - in CT26, and only 17% - in LLC model (Figure 9).

Thus, the efficacy of PDT with *meso*-tetra(3-pyridyl)bacteriochlorin with regard to small and large transplanted metastatic tumors is much more pronounced than the efficacy of PDT with Radachlorin®.

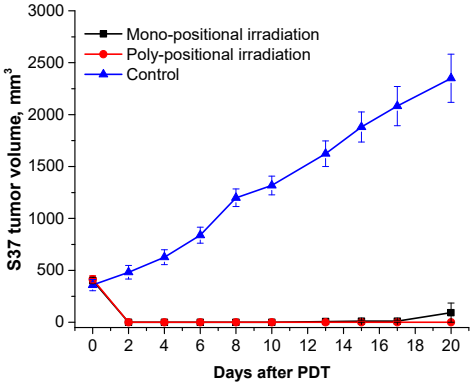

(**a**)

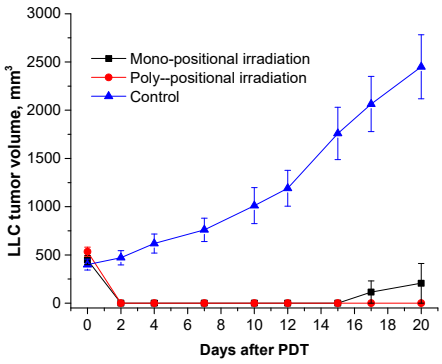

(**b**)

Preprints (www.preprints.org) | NOT PEER-REVIEWED | Posted: 9 November 2023 doi:10.20944/preprints202311.0582.v1

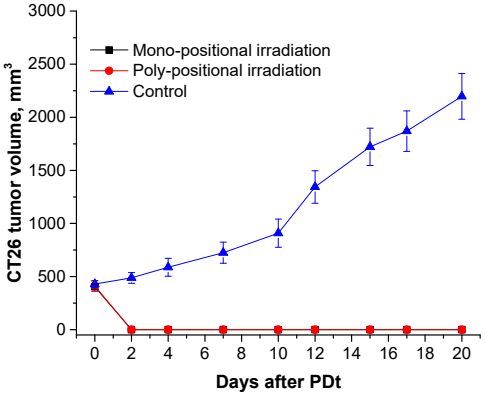

(**c**)

Figure 8. *Ex tempore* and further measured S37 (a), LLC (b), and CT26 (c) tumor volumes in mice treated with H_2Py_4BC-mediated PDT using mono- and poly-positional irradiation. PS dose of 2.0 mg/kg, 30 min interval between the PS infusion and irradiation.

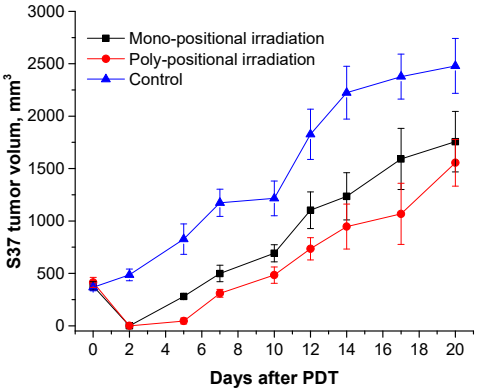

(**a**)

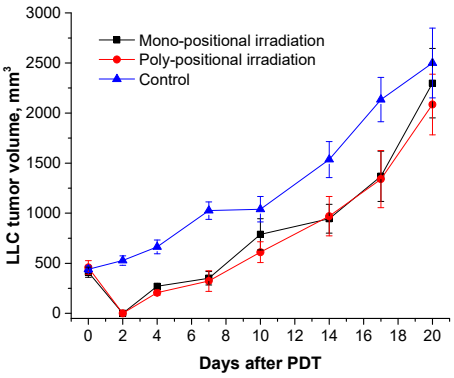

(**b**)

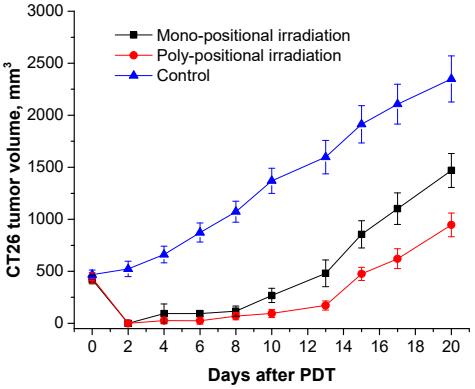

(**c**)

Figure 9. *Ex tempore* and further measured S37 (a), LLC (b), and CT26 (c) tumor volumes in mice treated with Radachlorin-mediated PDT using mono- and poly-positional irradiation. PS dose of 5.0 mg/kg, 15 min interval between the PS infusion and irradiation.

 doi:10.20944/preprints202311.0582.v1

2.3.3. Photoinduced antitumor activity of meso-tetra(3-pyridyl)bacteriochlorin and Radachlorin in the model of transplanted RS-1 rat liver tumor

Due to the metastatic character of murine transplanted tumors, the duration of observation of animals after PDT of large tumors until the forced euthanasia is applied (in accordance with humane guidelines) is not sufficient for the verification of its radical efficiency with regard to primary nodule. That is why RS-1 rat transplanted tumor was chosen for the comparative study of H_2Py_4BC and Radachlorin. The transverse dimensions of tumors at the time of the beginning of the exposure averaged 13.9x14.0x13.7 mm. The basis for the selection of PDT conditions in this animal model became the best regimen of those developed in the experiments in mice.

Neither visual nor palpation signs of the continued tumor growth in the rats from the experimental group were revealed during 180 days after the intravenous infusion of H_2Py_4BC in 1 mg/kg dose and subsequent poly-positional irradiation of the subcutaneous tumors with light of 747nm wavelength (total dose of 270 J/cm^2; TGI=100%, RR=100%). PDT of a large tumor performed with Radachlorin (2.5 mg/kg dose) absorbing light in the range with a 662 nm maximum did not demonstrate high efficacy. TGI did not exceed 30% for the entire period of the observation of the animals.

For the verification of the therapeutic effect, the sites of the impact were studied using MRI before and 25 days after the treatment in every rat from the group treated by PDT both with H_2Py_4BC (experimental group) and Radachlorin (control group). Histological analysis of the tissues after the photodynamic impact was also performed (Figure 10).

Before the treatment (Figure 10a,e,i), the subcutaneous RS-1 tumor graft looked like a massive formation of an alveolar-like structure surrounded by a thin connective tissue capsule. The tumor was well vascularized and despite its large volume had no signs of tumor tissue necrosis.

Histological examination of these areas revealed massive fibrosis, granulation tissue areas with sparse foci of lymphoid infiltration, as well as small clusters of siderophages. There were no signs of tumor growth in serial sections obtained from various tissue samples (Figure 10f,j).

In two other animals treated with H_2Py_4BC, MRI-images of the peripheral high density area in the impact region corresponding to scar changes contained small low density sites (Figure 10c).

Histological examination revealed that these residual defects corresponded to the foci of tumor tissue which preserved the cell structure similar to that of RS-1 (Figure 10g,k). At the same time, the remains of the tumor were as a rule surrounded by lymphoid infiltrate, and the nuclei of some tumor cells were destroyed.

The data obtained in experiments on transplantable tumors in rats and mice show obvious advantages of H_2Py_4BC in treating animals bearing large tumors in comparison with Radachlorin.

The results of histological studies suggest that the high efficacy of photodynamic treatment with the long wavelength photosensitizer against voluminous tumors takes place mostly due to the deeper penetration of the excitation light into the tumor tissue.

Preprints (www.preprints.org) | NOT PEER-REVIEWED | Posted: 9 November 2023 doi:10.20944/preprints202311.0582.v1

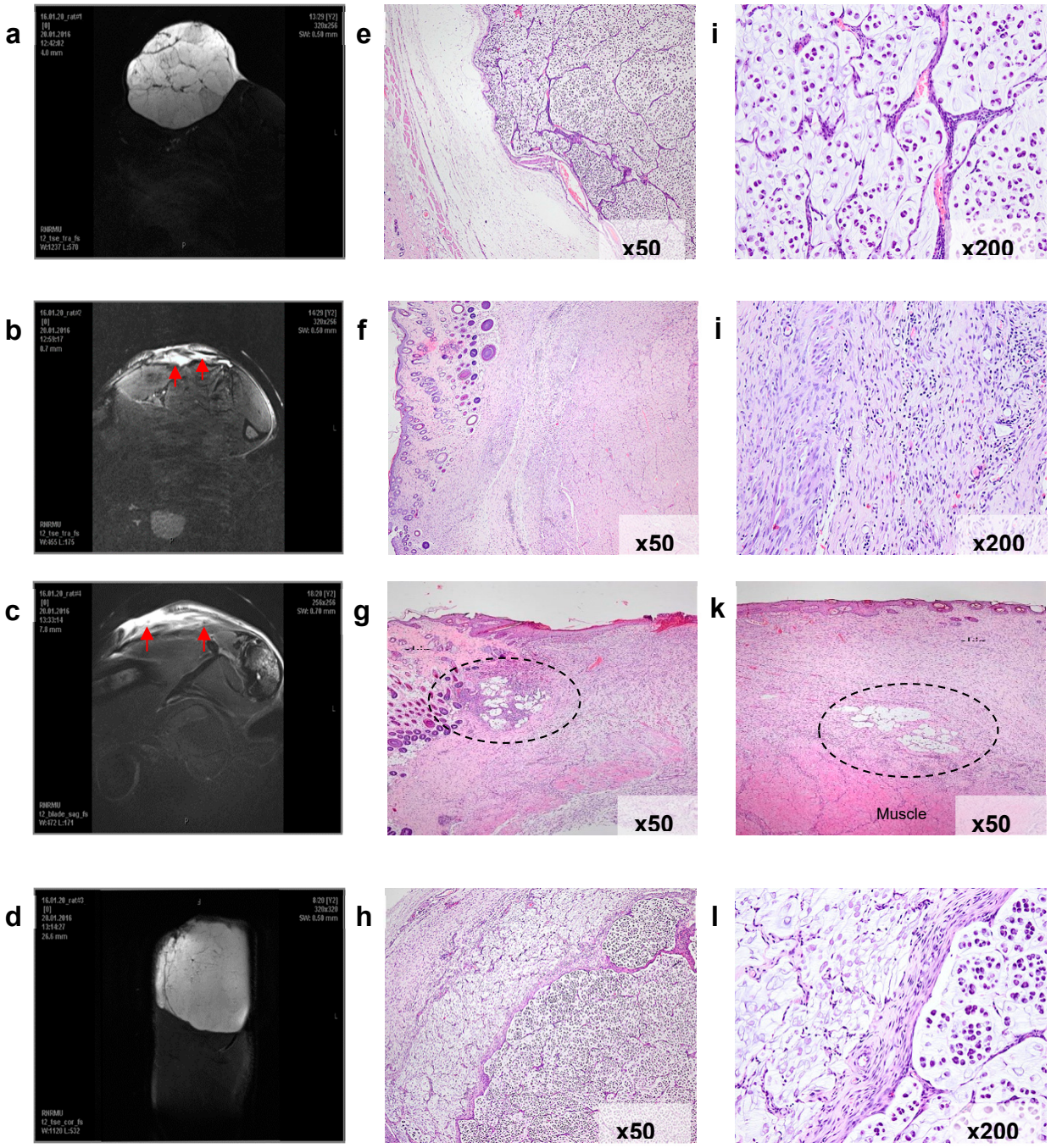

Figure 10. Verification of PDT efficacy in the model of subcutaneously transplanted RS-1 tumor in rats. Frontal magnetic resonance imaging (MRI) scans of the animals' paws with the transplanted tumors (*a - d*) and microphotographs of histological sections of the tissues in the corresponding sites (*e –l*, optical microscope magnification is indicated). *a, e, i* – a representative tumor node before PDT treatment. The tumor consists of irregular alveolar-like mucinous structures separated by fibroconnective septae and containing signet ring cancer cells. *b, f, j* –complete tumor eradication in 25 days after $H_2$3PyBc-mediated PDT (animal №1). The arrow on the MRI scan indicates a high-density area corresponding to fibrotic changes in the irradiated zone. Histological examination revealed granulation tissue and fibrosis only, the tumor cells were absent. *c, g, k* –partial tumor eradication in 25 days after $H_2$3PyBc-mediated PDT (animal №2). The arrows on the MRI scan indicate the periphery of the irradiated zone, where two small residual foci of the tumor cells in the fibrotic connective tissue were found during the histological examination. *d, h, l* –continued tumor growth in 25 days after PDT with Radachlorin. The massive tumor node under the thin high-density layer of the

Preprints (www.preprints.org) | NOT PEER-REVIEWED | Posted: 9 November 2023 doi:10.20944/preprints202311.0582.v1

damaged tissue can be seen on the MRI scan. Histological images demonstrate necrotic changes in the irradiated zone (left) and underlying live tumor tissue (right).

3. Materials and Methods

3.1. Photosensitizers

H_2Py_4BC has been synthesized in a two-step procedure from pyrrole and 3-pyridine aldehyde (Scheme 1). The intermediate *meso*-tetra(3-pyridyl)porphyrin was prepared by acetic acid catalyzed condensation of equimolar amounts of pyrrole and 3-pyridine aldehyde in aerobic conditions. Its reduction with diimide generated from the thermal decomposition of p-toluenesulfonylhydrazine in the presence of anhydrous potassium carbonate in dry pyridine afforded H_2Py_4BC. The UV-Vis spectrum of H_2Py_4BC in $CHCl_3$ contains two intense bands in the visible and NIR spectral region at 521 and 747 nm (lgε 4.71 and 5.05, respectively), which represent the split Q band, and split B band at 357 and 380nm (lgε 5.00 and 5.08, respectively) in the UV spectral region, typical for bacteriochlorin derivatives [21].

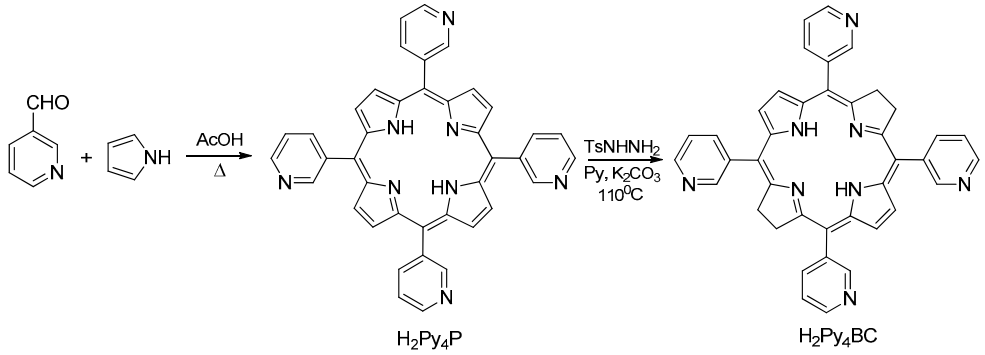

Scheme 1. The scheme of the synthesis of meso-tetra(3-pyridyl)bacteriochlorin.

For *in vitro* and *in vivo* studies, hydrophobic H_2Py_4BC was solubilized in 4% dispersion of Kolliphor ELP (BASF, Germany). H_2Py_4BC and Kolliphor ELP were dissolved in chloroform and the solution was heated to 40–55°C in 1 L round bottom flask equipped with magnetic stirrer. The solvent was removed in vacuum in the rotary evaporator (IR-1M2) at the water bath of 30–40 °C temperature. The formed film further was thoroughly dried in vacuum and then hydrated by adding 10 ml of phosphate buffer solution (PBS) with pH = 7.34. The stirring was continued till complete film dissolution. The obtained H2Py4BC solution was filtered through 0.22 μm pore size membrane filter (Millipore, Type GS). All procedures were performed under dimly lit conditions. The resultant stock solution of H_2Py_4BC in 4% Cremophor (0.4 mg/ml) was stored at 6–10 °C in the dark.

Radachlorin® 0.35% solution for intravenous administration was obtained from RadaPharma (Russia). This photosensitizer is a modified mixture of the natural chlorins extracted from microalgae of *Spirulina* and containing 70–90% chlorin e6 with the fluorescence maximum at 662 nm. The medicine was stored in the dark at 4–10° C [27].

3.2. Spectroscopy

For the spectrophotometric study the stock H_2Py_4BC solution was diluted in 0.9% aqueous sodium chloride (NaCl) to the final concentration of 0.5μg/ml. The absorption spectra were measured at 300 to 900 nm with Genesys 2 (USA) spectrophotometer.

Fluorescence measurements were performed using local fluorescence spectroscopy (LFS) technique with the LESA-06 (Biospec, Russia) laser spectrum analyzer. Fluorescence was excited by 632.8 nm radiation from He-Ne laser. Fluorescence spectra were measured *ex tempore,* as well as after 1- and 6-month incubation in the dark at 6-10°C.

 doi:10.20944/preprints202311.0582.v1

3.3. In vitro studies

Both human tumor cell cultures (HEp2 epidermoid carcinoma and EJ bladder carcinoma) and mouse tumor cell cultures (S37 sarcoma, Lewis lung carcinoma (LLC), and CT26 colon carcinoma) were used in the study. HEp2, EJ, and S37 cell cultures were obtained from D.I. Ivanovskiy Institute of Virology, RAS; LLC cell culture was obtained from ECACC; CT26 cell culture was obtained from ATCC. Eagle's minimal essential medium (EMEM) and Dulbecco's Modified Eagle's Medium (DMEM) supplemented with L-glutamine, 10% fetal calf serum (FCS, PanEco, Russia), and gentamicin (Biochemist, Russia) were used for cell culturing.

For the experiments, cells were seeded in 96-well plates (Costar, USA) in the amount of $7x10^3$ cells per well. H_2Py_4BC solution in complete culture medium was added to the wells 24 hours after cell seeding in the final concentrations of 10 nM to 2400 nM in triplets. Duration of incubation with the cells prior to exposure to light varied from 30 minutes to 6 hours. Light exposure was performed at a dose of 10 J/cm^2 in two variations: in the presence of the dye in the incubation medium and after replacing the contents of the wells prior to irradiation for the medium without PS. After completing irradiation the cells were incubated in 5% CO_2 atmosphere for 24 hours. In order to eliminate the dark toxicity of the dye other set of the cells was incubated with H_2Py_4BC in the dark under the same conditions as irradiated cells. Control cells were not exposed to the PS or light. Cell viability was assessed using the colorimetric MTT assay. MTT results were used to calculate the IC_{50} value (PS concentration which caused 50% cell death after the irradiation). Three independent tests were used for calculation of the quantitative parameters.

3.4. In vivo studies

3.4.1. Animals

BALB/c and F1 mice (female, 7-9 weeks old, 18-20 g body weight) and inbred rats (female, 6-8 weeks old, 120-150 g body weight) were obtained from "Andreevka" nursery of laboratory animals (Russia). Mice and rats were kept in separate rooms, in the controlled environment.

All of the animals were admitted with a veterinary passport and a certificate of quality. All procedures for routine animal care were performed in accordance with standard operational procedures and the sanitary guidelines for the design, equipment, and maintenance of experimental biological clinics and the Laboratory Animals manual [28–30].

3.4.2. Tumor models

The experiments were performed using the models of transplanted syngeneic tumors in mice and rats.

S37 sarcoma (lymphogenous metastasis pathway with location of metastasis in lymph nodes and 100% frequency of metastasis formation [31]) S37 strain was maintained in ascitic form in ICR male mice (CD-1). For the experiments, tumor cells isolated from ascitic fluid were inoculated subcutaneously to F1 mice in the right thigh in the amount of 1.0×10^6 cells per mouse.

Lewis adenocarcinoma (LLC; hematogenous metastasis pathway with location of metastasis in lungs and 100% frequency of metastasis formation). LLC strain was maintained in the solid form in C57BL/6 male mice. For the experiments, 10 mg of the crushed tumor tissue were transplanted subcutaneously on the outer side of the thigh of F1 mice.

CT26 colon carcinoma (hematogenous metastasis pathway with location of metastasis in lungs and 100% frequency of metastasis formation). CT26 cells were cultured *in vitro* and inoculated subcutaneously on the outer side of the thigh of BALB/c mice in the amount of 0.5×10^6 cells per mouse.

RS-1 cholangiocellular carcinoma (non-metastatic tumor). RS-1 strain was maintained in solid form in inbred male rats. For the experiments, 30 mg of crushed tumor tissue were transplanted on the outer side of the thigh.

 doi:10.20944/preprints202311.0582.v1

3.4.3. Biodistribution of meso-tetra (3-pyridyl) bacteriochlorin

The study of H_2Py_4BC biodistribution was performed in mice with inoculated tumors. H_2Py_4BC was infused intravenously in the dose of 2.5 mg/kg. The evaluation of its biodistribution was performed by optic imaging method in S37 model, as well as by *ex vivo* method of local fluorescence in S37, LLC, and CT26 models.

Intravital integral fluorescence images of the animal bodies were recorded with IVIS Spectrum-CT device (PerkinElmer) in dynamics at 0.25, 0.5, 1, 2, 4, and 24 hours after intravenous administration of PS in 2.5 mg/kg dose. Animals were narcotized using the mixture with 2% content of isofluran (Abbott, USA) before the investigation. Fluorescence excitation was performed at 710 nm wavelength. Spectral analysis using LivingImage 4.4 software (Perkin Elmer) was performed to separate the fluorescence signals of the fluorophore and the tissue. Fluorescence intensity was measured in photons / sec / cm^2.

Fluorescence measurements were performed by local fluorescence spectroscopy (LFS) technique with the LESA-06 laser spectrum analyzer (Biospec, Russia). Mice were sacrificed by decapitation at various time intervals (ex tempore, at 0.08, 0.25, 0.5, 2, 4, 24, 48, 120, and 168 hours) after PS administration, and blood was collected. Animals were necropsied, and *ex vivo* fluorescence was recorded in the blood, tumor tissue, skin, muscle, kidney, and spleen in the spectral range of 640-800 nm. Each experimental group of all observation times consisted of three animals.

Integral fluorescence intensity from the collected tissue samples at 747 nm corresponding to λ_{max} of PS fluorescence was normalized to the integral fluorescence intensity of the excitation laser light diffusely back-scattered from the tissue, giving normalized fluorescence (NF). The fluorescence contrast (FC) was calculated as the ratio of an average NF in the tumor versus the skin.

3.4.4. Photodynamic therapy with meso-tetra (3-pyridyl) bacteriochlorin and Radachlorin in the models of mice and rats with transplanted tumors

The anti-tumor efficacy of PDT with H_2Py_4BC was studied using S37, CT26, and LLC murine tumors and RS-1 rat tumor. Every experimental group consisted of 5 animals.

Mice were exposed to PDT 6-7 and 12-14 days post tumor cell inoculation, and mean volumes of tumor nodes in these periods were 130±20 mm^3 and 460±40 mm^3, respectively. Animals were anesthetized by intraperitoneal injection of droperidol (solution for injections, 2.,5 mg/ml, Russia) 10 or 15 min before the PDT session.

H_2Py_4BC or Radachlorin® was infused intravenously. Irradiation was performed using diode device (Russia) consisting of a light source, an optic homogenizer in the form of octagonal rectangular prism, a light emission power regulator (30 to 150 mW/cm^2), and a LED current indicator. For PDT with H_2Py_4BC a light source with 740 ± 28 nm wavelength was used, whereas for PDT with Radachlorin® the source with 662±14 nm wavelength. PS dose, time interval between the dye infusion and the beginning of irradiation, and light dose varied for the sake of choosing optimal treatment conditions (see "Results"). Group of animals without treatment served as the control group.

Mono-positional regimen was used for irradiation of small tumors (single irradiation field, light dose of 90 J/cm^2), whereas for irradiation of bulky tumors the following regimens were used: single irradiation field and light dose of 270 J/cm^2 or poly-positional regimen (three interfering fields with 90 J/cm^2 light dose for each one and 270 J/cm^2 total light dose).

RS-1 bearing rats were exposed to PDT 13-14 days post tumor cell inoculation when the mean volume of tumor nodules reached 1400±100 mm^3. All rats were anesthetized with the combination of zoletil 100 (VirbacSanteAnimale, France) and xylazine 2% (InterchemieWerken de Adelaar@, Netherlands) administered intraperitoneally 10 or 15 min before PDT. H_2Py_4BC or Radachlorin were infused intravenously. Dye doses were calculated with regard to the murine therapeutic doses and the conversion factor for rats equal to 5.9 (1.0 mg/kg dose for H_2Py_4BC and 2.5 mg/kg dose for Radachlorin), and the most efficient conditions of irradiation developed in the experiments on murine models were implemented. The irradiation was performed using LED sources with the corresponding wavelength under poly-positional regimen (total light dose of 270 J/cm^2).

 doi:10.20944/preprints202311.0582.v1

3.4.5. Evaluation of anti-tumor efficacy

The presence of tumor nodules and their volumes were determined during the observation. Tumor measurements began 3 or 4 days after PDT when the edema decreased. Tumor volume was estimated as $V = d_1 \times d_2 \times d_3 \times 0.52$, where d_1, d_2, and d_3 were three orthogonal diameters of the tumor nodule.

The progressive worsening of animals' condition due to the growth of the primary or metastatic tumors was the indication for euthanasia and was considered to be the end point of the observation. Euthanasia in mice was performed when tumors reached the volume of 2000 to 2500 mm^3 and in rats when tumors reached the volume of 4500 to 5000 mm^3. Mice without visual and palpable tumor growth were observed for 90 days and rats for 180 days. After these periods the animals were euthanized, dissected, and the areas of inoculated tumors (primary nodules) and the lymph nodes or lungs (metastatic nodules) were evaluated. Animals without signs of tumor growth at the end point of the observation were considered to be cured. Efficacy factors for the study included:

inhibition of tumor growth, $(ITG) = [(V_c - V_e)/V_c] \times 100\%$, where V_e and V_c are mean tumor volumes in the treated tumor-bearing mice and control tumor-bearing mice, respectively;

response rate $(RR) = [N_c/N_t] \times 100\%$, where N_c is the total number of cured animals and N_t is the total number of treated animals [29].

ITG ≥ 70%, RR ≥ 25% were set as biologically significant.

3.4.6. Magnetic resonance imaging (MRI)

MR imaging of rats was performed with BioSpecClinScan 7T 70/30 (BrukerBiospin, Germany) on the day of irradiation (13th or 14th day of the tumor growth) and on the 25th day after PDT.

3.4.7. Histological analysis

Tissues for histological analysis were fixed with 10% neutral buffered formalin and after the standard histological processing were embedded into paraffin. Serial tissue sections (4 μm thick) were stained with hematoxylin and eosin.

3.4.8. Statistics

U-Mann-Whitney criteria was used to evaluate the differences of the quantitative parameters between the groups. The calculations were performed using Statistica 8.0 (StatSoft, Inc., USA). The difference was considered to be significant at $p < 0.05$.

4. Conclusions

Meso-tetra(3-pyridyl)bacteriochlorin studied in this work is the novel synthetic photosensitizer for PDT of malignant tumors which absorbs at 747 nm (in the long wavelength region of the spectrum) and is stable for 6 months when stored in the dark. H_2Py_4BC demonstrates pronounced photoinduced activity *in vitro* against tumor cells of various genesis (IC_{50} is 32.0±2.0 nM for HEp2, 35.2±2.4 nM for EJ, 68.2±1.6 nM for S37, 21.4±1.4 nM for CT26, and 21.6±1.5 nM for LLC) without dark toxicity.

This photosensitizer quickly penetrates and is accumulated in S37, CT26, and LLC tumors as well as in inner organs of mice (within 5 to 30 minutes). The normalized fluorescence in tumors remains high up to 2 hours. In 24 hours after infusion 80% of the dye excreted from skin and 87% - 92% from the liver, kidneys, and spleen. The residual amount of H_2Py_4BC could be detected in liver up to 5 days.

PDT with meso-tetra(3-pyridyl)bacteriochlorin demonstrates high antitumor activity in mice and rats bearing both small or large tumors. Its efficacy significantly exceeds that of PDT with Radachlorin (662 nm absorption maximum) as confirmed by well-known experimental oncology criteria, and also by MRI and histological analysis.

5. Patents

Yakubovskaya, R.I., Lukyanets, E.A., Vorozhtsov, G.N., Makarova E.A., Morozova, N.B., Makarova, E.A., Lastovoy, A.P., Plotnikova, E.A. Photosensitizer for photodynamic therapy. Patent rus №2549953

Author Contributions: Conceptualization, E.P. and A.P.; methodology, E.P., E.N., and M.A.; software, E.P.; formal analysis, A.P; investigation, E.P., M.A.; resources A.P., P.S., and A.K., data curation, E.P. and E.N.; writing—original draft preparation, E.P.; writing—review and editing, A.P., P.S., A.K. and E.N.; visualization, E.P. and M.A.; supervision, A.P.; project administration, E.N., A.P., P.S., and A.K. All authors have read and agreed to the published version of the manuscript.

Funding: This research received no external funding.

Institutional Review Board Statement: All manipulations with animals were approved by the Committee of the National Medical Research Radiology Centre of the Ministry of Health of the Russian Federation for bioethical control over the maintenance and use of laboratory animals for scientific purposes (Minutes No. 61 dated 14 November 2016), and performed in accordance with the national and international rules for the humane treatment of animals (European Convention for the Protection of Vertebrate Animals Used for Experimental and Other Scientific Purposes, Council of Europe(ETS 123), Eighth Edition of the Guide for the Care and Use of Laboratory Animals (NRC 2011)). All materials, methods, and experimental procedures where animals were used were described in accordance with ARRIVE rules [32].

Informed Consent Statement: Not applicable.

Data Availability Statement: The data presented in this study are available from the authors on request.

Conflicts of Interest: The authors declare no conflicts of interest.

References

1. Kou, J., Dou, D., Yang, L. Porphyrin photosensitizers in photodynamic therapy and its applications. *Oncotarget* **2017**, 8, 81591–603. https://doi.org/10.18632/oncotarget.20189
2. Mironov, A.F. Antitumor photodynamic therapy – a novel efficient method for diagnostics and therapy of malignant tumors. *Soros Educational Journal* **1996**, 8, 32-40.
3. Yakubovskaya, R.I., Morozova, N.B, Pankratov, A.A. et al. Experimental photodynamic therapy: 15 years of development. *Russian Journal of General Chemistry* **2015**, 85, 217-239. doi: 10.1134/S1070363215010405.
4. Moghissi, K., Dixon, K., Gibbins S. A surgical View of Photodynamic Therapy in oncology: a review. *The surgery Journal* **2015**, 01, 1-15. doi: 10.1055/s-0035-1565246.
5. Lange, C., Bednarski, P. Photosensitizers for Photodynamic Therapy: Photochemistry in the Service of Oncology. *Curr Pharm Des*. **2016**, 22, 6956-6974. doi: 10.2174/1381612822666161124155344.
6. O. I. Koifman, T. A. Ageeva, N. S. Kuzmina et al. Synthesis Strategy of Tetrapyrrolic Photosensitizers for Their Practical Application in Photodynamic Therapy. *Macroheterocycles* **2022,** 15 (4), 207-302. DOI: 10.6060/mhc224870k
7. Pantyushenko I.V., Grin M.A., Yakubovskaya R.I., Plotnikova E.A., Morozova N.B., Tsygankov A.A., Mironov A.F. The novel highly effective ir-photosensitizer for photodynamic therapy of cancer. *Fine Chemical Technologies*. **2014**; 9(3), 3-10.
8. Gloria Mazzone, Marta E. Alberto, Bruna C. De Simone, Tiziana Marino and Nino Russo. Can Expanded Bacteriochlorins Act as Photosensitizers in Photodynamic Therapy? Good News from Density Functional Theory Computations. *Molecules* **2016**, 21, 288. DOI:10.3390/molecules21030288.
9. Filonenko, E.V. Clinical implementation and scientific development of photodynamic therapy in Russia in 2010–2020. *Biomed. Photonics* **2021**, 10, 4–22.
10. Li, X., Lovell, J.F., Yoon, J. *et al.* Clinical development and potential of photothermal and photodynamic therapies for cancer. *Nat Rev Clin Oncol* **2020**, **17**, 657–674. DOI:10.1038/s41571-020-0410-2.
11. Azzouzi, A.R, Barret, E., Moore, C.M., Villers, A., Allen, C., Scherz, A., Muir, G.W., Wildt, M., Barber, N.J., Lebdai, S., Emberton, M. TOOKAD(®) Soluble vascular-targeted photodynamic (VTP) therapy: determination of optimal treatment conditions and assessment of effects in patients with localised prostate cancer. *BJU In.* **2013**, 112, 766-774. DOI:10.1111/bju.12265

12. Azzouzi, A.R., Barret, E., Bennet, J., Moore, C.M., Taneja, S.S., Muir, G., Villers, A., Coleman, J.A., Allen, C., Scherz, A., Emberton, M. TOOKAD® Soluble focal therapy: pooled analysis of three phase II studies assessing the minimally invasive ablation of localized prostate cancer. *World J Urol*. **2015**, 33, 945-953. doi:10.1007/s00345-015-1505-8.
13. Gomes-da-Silva, L.C., Zhao, L., Bezu, L., Zhou, H., Sauvat, A., Liu, P., Durand, S., Leduc, M., Souquere, S., Loos, F., Mondragon, L., Sveinbjornsson, B., Rekdal, O., Boncompain, G., Perez, F., Arnaut, L.G., Kepp, O., Kroemer, G. Photodynamic therapy with redaporfin targets the endoplasmic reticulum and Golgi apparatus. *EMBO J.* **2018**, 37, 98354. doi: 10.15252/embj.201798354.
14. Baskaran, R., Lee, J. and Yang, S.-G. Clinical development of photodynamic agents and therapeutic applications. Biomaterials Research 2018, 22, 1-8. doi: 10.1186/s40824-018-0140-z.
15. Santos, L.L., Oliveira, J., Monteiro ,E., Santos, J., Sarmento, C. Treatment of Head and Neck Cancer with Photodynamic Therapy with Redaporfin: *A Clinical Case Report. Case Rep Oncol*. **2018**, 11, 769-776. DOI: 10.1159/000493423.
16. Malwina Karwicka, Barbara Pucelik, Michał Gonet, Martyna Elas & Janusz M. Dąbrowski. Effects of Photodynamic Therapy with Redaporfin on Tumor Oxygenation and Blood Flow in a Lung Cancer Mouse Model. *Scientific Reports* **2019**, 9, 12655. DOI: 10.1038/s41598-019-49064-6
17. Dudkin, S.V., Makarova, E.A., Slivka, L.K., Lukyanets, E.A. Synthesis and properties of tetra- and octacationic meso-tetrakis(3-pyridyl)bacteriochlorin derivatives. *J. Porphyrins Phthalocyanines* 2014, 18, 107-114. DOI: 10.1142/S1088424613501162.
18. Nevonen, D.E., Makarova, E.A., King, A., Lukyanets, E.A. Nemykin, V.N. Elucidation of the Electronic Structure of Water-Soluble Quaternized meso-Tetrakis(3-pyridyl)bacteriochlorin Derivatives by Experimental and Theoretical Methods. *J. Porphyrins Phthalocyanines* **2018**, 22, 965-971. DOI: 10.1142/S1088424618500980.
19. Yakubovskaya, R.I., Plotnikova, E.A., Plutinskaya, A.D., Morozova, N.B., Chissov, V.I., Makarova, E.A., Dudkin, S.V., Lukyanets, E.A., Vorozhtsov, G.N. Photophysical properties and in vitro and in vivo photoinduced antitumor activity of cationic salts of meso-tetrakis(N-alkyl-3-pyridyl)bacteriochlorins. *J. Photochem. Photobiol. B. Biol*. **2014**, 130, 109–114. DOI: 10.1016/j.jphotobiol.2013.10.017.
20. Dudkin, S.V., Efremenko, A.V., Ignatova, A.A., Kobzeva, E.S., Lukyanets, E.A., Makarova, E.A., Morozova, N.B., Plutinskaya, A.D., Feofanov, A.V., Chissov, V.I., Yakubovskaya, R.I. Photosensitizer for photodynamic therapy. Patent rus №2476218 2012.
21. Yakubovskaya, R.I., Lukyanets, E.A., Vorozhtsov, G.N., Makarova E.A., Morozova, N.B., Makarova, E.A., Lastovoy, A.P., Plotnikova, E.A. Photosensitizer for photodynamic therapy. Patent rus №2549953 2015.
22. Bezulenko, V.N., Kalinichenko A.N., Kobzeva, E.S., Lukyanets E.A., Makarova E.A., Morozova, N.B., Plotnikova, E.A., Plutinskaya, A.D., Starkova, N.N., Stramova, V.O., Yakubovskaya, R.I. Water soluble dosage form of meso-tetra(3-pyridyl)bacteriochlorin for photodynamic therapy. Patent rus №2663900 2017.
23. Makarova, E.A., Lukyanets, E.A., Tiganova, I.G., Romanova, Y.M., Meerovich, G.A., Loschenov, V.B., Alekseeva, N.V., Akhlyustina, E.V. Photosensitizers for Photodynamic inactivation of pathogenic bacteria including in biofilms. RU Patent 2670201 2018
24. Meerovich, G.A., Akhlyustina, E.V., Tiganova, I.G., Makarova, E.A., Alekseeva, N.V., Romanishkin, I.D., Philipova, N.I., Lukyanets, E.A., Gonchukov, S.A., Romanova, Ju.M., Loschenov, V.B. Photosensitizers for antibacterial photodynamic therapy based on tetracationic derivatives of synthetic bacteriochlorins. *Laser Phys. Lett*. **2018**, 15, 115602. DOI: 10.1088/1612-202x/aae03f.
25. Meerovich, G.A., Akhlyustina, E.V., Tiganova, I.G., Lukyanets, E.A., Makarova, E.A., Tolordava, E.R., Yuzhakova, O.A., Romanishkin, I.D., Philipova, N.I., Zhizhimova, Yu.S., Romanova, Yu.M., Loschenov, V.B., Gintsburg, A.L. Novel polycationic photosensitizers for antibacterial photodynamic therapy. *Adv. Exp. Med. Biol*. **2019**, 1–19. DOI: 10.1007/5584_2019_43.
26. Akhlyustina, E.V., Meerovich, G.A., Tiganova, I.G., Makarova, E.A., Philipova, N.V., Romanishkin ,I.D., Alekseeva, N.V., Lukyanets, E.A., Romanova, Yu.M., Loschenov, V.B. New cationic photosensitizers: photophysical properties and results of preliminary studies of antibacterial efficacy. J. Phys.: Conf. Ser. **2019**, 1189, 012033. DOI: 10.1088/1742-6596/1189/1/012033.
27. https://www.rlsnet.ru/drugs/radaxlorin-21189.
28. Guide to Laboratory Animals and Alternative Models in Biomedical Research, Karkishchenko, N.N.; Grachev, S.V. (Eds.) *Profil*: Moscow, Russian, **2010**; 358. (In Russian).

29. Guidelines for Conducting Preclinical Studies of Drugs. Part 1. Mironov, A.N. (Ed.) Grif and K: Moscow, Russian, **2012**; 657–671. (In Russian)
30. Directive 2010/63/EU of the European Parliament and of the Council of 22 September 2010 on the Protection of Animals Used for Scientific Purposes. Official Journal of the European Union, 10 October **2010**. Available online: https://eur-lex.europa.eu/
31. Morozova, N.B., Andreeva, T.N., Karmakova, T.A., Rubcova, N.A., Yakubovskaya, R.I., Chissov, V.I., Belenkov, Yu.N., Gulyaev, N.V., Pirogov, Yu.A. Usage of magnetic resonance imaging for evaluation of S37 sarcoma metastasis in mice. *Medical Physics* **2013**, 1, 38-43.
32. Percie du Sert, N.; Hurst, V.; Ahluwalia, A.; Alam, S.; Avey, M.T.; Baker, M.; Browne, W.J.; Clark, A.; Cuthill, I.C.; Dirnagl, U.; et al. The ARRIVE Guidelines 2.0: Updated Guidelines for Reporting Animal Research. *Exp. Physiol*. **2020**, 105, 1459–1466.